4th International Conference on Experiments/Process/System Modeling/Simulation/Optimization
4th IC-EpsMsO
Athens, 6-9 July, 2011

Segmentation and Classification of Histopathology Images for Abetting Diagnosis in Urinary Bladder Cancer

Christos Sakellarios[1], Spiros Kostopoulos[2], Dimitris Glotsos[2], Panagiota Ravazoula[3] and Dionisis Cavouras[2]

[1] Department of Informatics and Telecommunications, University of Athens, Greece
e-mail: chsakell@hotmail.com
[2] Medical Image and Signal Processing Laboratory, Department of Medical Instruments Technology, Technological Educational Institute of Athens, 12210, Egaleo, Athens, Greece
web page: http://www.teiath.gr/stef/tio/medisp/index.htm
[3] Department of Pathology, University Hospital of Patras, Patras, Greece

Keywords: Image Analysis, Pattern Recognition, Urinary Bladder Cancer, Histopathology

Abstract. *The present study proposed an automated computer-based system, which discriminates low from high malignancy urinary bladder tumours, based on morphological and textural features come from nuclei, on microscopy tissue slides. An experienced pathologist assessed fifty six biopsy tissues from urinary bladder cancer stained with Hematoxylin and Eosin, according to the latest WHO/ISUP grading system. Thirty seven cases were categorized as low grade and nineteen as high grade. Tissue slides were digitized and images were segmented, based on a fuzzy c-means clustering algorithm, to nuclei and surrounding tissue regions. Thirty four textural and morphological features were extracted from nuclei and their values were averaged to represent the cases. Based on those features, a pattern recognition system was designed, implemented and evaluated capable of classifying the cases into low or high grade categories. The efficiency of five different classifiers and their combination in an ensemble scheme was evaluated. The proposed system achieved over 89% overall classification accuracy between low and high grade malignancy.*

1 INTRODUCTION

Urinary bladder cancer is an heterogeneous disease with complex history in diagnosis. In west world, it is the forth most common malignancy for men and eighth for women [1]. In Europe and United States, it reaches 5%-10% incidence rate over all kind of malignancy of men population. The probability of occurring bladder cancer after the age of 75 is 2%-4% for men and 0.5%-1% for women [2-3]. According to the consensus of World Health Organisation and International Society of Urologic Pathologists (WHO/ISUP), bladder cancer is classified as well, moderate and poorly differentiated carcinoma, which describes low and high grade malignancy [4,5].

Digital image analysis and pattern recognition systems have been previously proposed for detecting neoplastic changes at their early stages and monitoring urinary bladder cancer progression and regression in the course of therapy management [6-9]. Those studies proposed a variety of computer-based systems and image analysis techniques, in order to characterize microscopy tissue slides of urinary bladder cancer. Chaudhuri et al. [6] and Young et al. [7], described techniques for characterizing microscopy images by modeling tissue's cell organization. Choi et al. [8] and Jarkans et al. [9] developed computer-based systems taking into account morphological and textural features. Numerous studies [10-17] concluded that nuclei features, like shape, area or texture, exhibit high diagnostic value. Consequently, nuclei segmentation and feature extraction is a crucial step in those systems. Several studies have proposed different algorithms for image segmentation and nuclei extraction. Some of those used threshold methods [9,12], while others applied pixel-based pattern recognition techniques [18,19]. Spyridonos et al. [19], proposed a system, based on Artificial Neural Network for both segmentation and classification. More recently, Glotsos et al. [20] performed image segmentation by combining Support Vector Machine Clustering and Active Contour models.

In the present study, a pattern recognition system is proposed for classification of urinary bladder cancer in low and high grade malignancy. An efficient method for nuclei segmentation is proposed based on a fuzzy c-means clustering algorithm and five different classifiers, which were tested and combined in an ensemble multi-classifier scheme. Moreover, the system was evaluated for its performance in unseen data.

2 MATERIALS AND METHODS

Fifty six (56) tissue sections of bladder cancer were collected from the Department of Pathology, University Hospital of Patras, Greece. Tissue samples were formalin fixed, paraffin embedded and were stained with Hematoxylin-Eosin. All cases were assessed for their histological tumour grade (low-high) by an experienced pathologist (P.R.), according to the WHO/ISUP grading system. All tissues slides were digitized in 562x766x8bit resolution by a Zeiss KF2 microscope with an Ikegami video camera attached on it.

2.1 Segmentation

The aim of segmentation was to distinguish nuclei from the surround tissue (background). Digitized images (Figure 1a) were firstly converted to greyscale format (Figure 1b), since the present work did not account for the colour information. A Gaussian filter (σ=0.5, size: 7x7), was applied to reduce noise effect on the image (Figure 1c). Then, image segmentation was performed by a fuzzy c-means (FCM) clustering algorithm, indicating that there are 3 different variations (c=3 clusters) of greyscale, which resulted in a binary image (Figure 1d), where background appeared in black and nuclei in white colour. FCM is a method of clustering, which allows a particular pixel to belong to one or more clusters with different degree (fuziness) [21,22]. It is based on minimization of the following objective function (eq. 1):

$$J_m = \sum_{i=1}^{N} \sum_{j=1}^{C} u_{ij}^{m} \left\| x_i - c_j \right\|^2 \quad , \quad 1 \le m < \infty \tag{1}$$

where m is any real number greater than 1, u_{ij} is the degree of membership of x_i in the cluster j, x_i is the ith of d-dimensional measured data, c_j is the d-dimension center of the cluster, and ||*|| is any norm expressing the similarity between any measured data and the center. Fuzzy partitioning is carried out through an iterative optimization of the objective function shown above, with the update of membership u_{ij} and the cluster centers c_j by equations 2 and 3 respectively.

$$u_{ij} = \frac{1}{\sum_{k=1}^{C} \left(\frac{\left\| x_i - c_j \right\|}{\left\| x_i - c_k \right\|} \right)^{\frac{2}{m-1}}} \tag{2}$$

$$c_j = \frac{\sum_{i=1}^{N} u_{ij}^{m} \cdot x_i}{\sum_{i=1}^{N} u_{ij}^{m}} \tag{3}$$

Algorithm terminates when equation 4 is satisfied:

$$\left\| J_{m+1} - J_m \right\| < \varepsilon \tag{4}$$

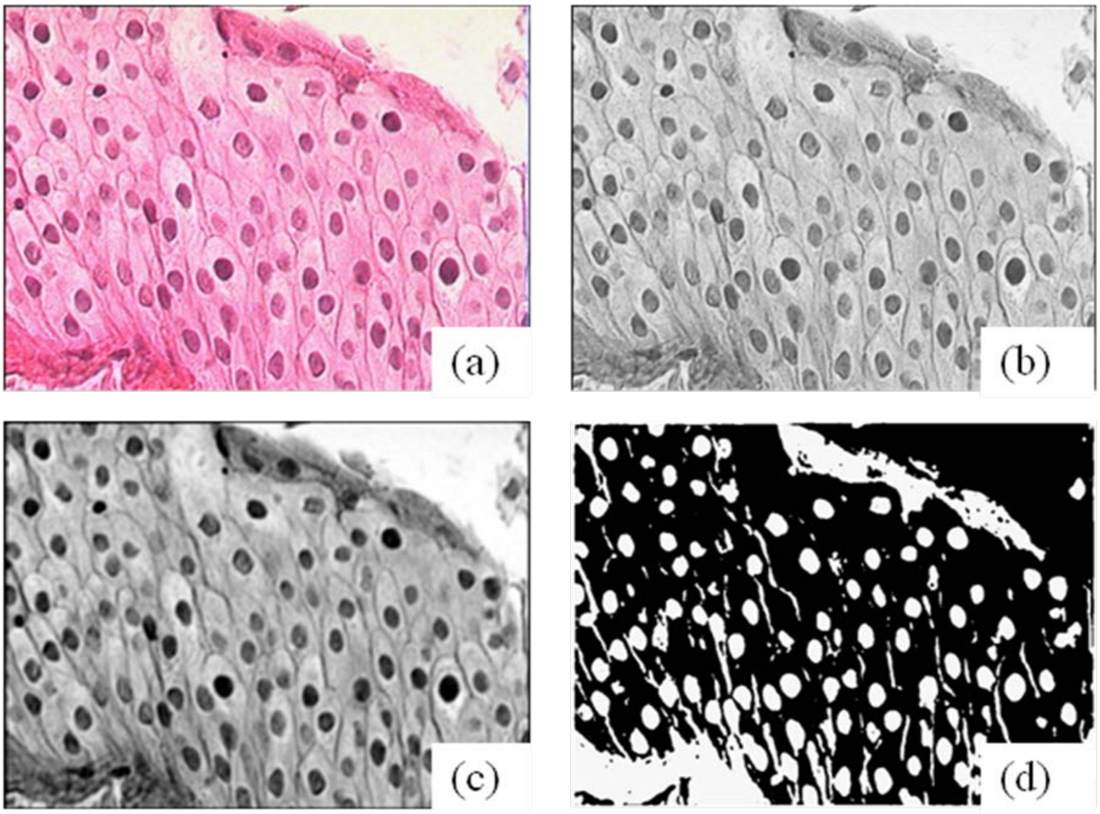

Figure 1. (a) Digitized RGB image, (b) Greyscale converted image, (c) Denoised image with Gaussian filter, (d) Segmented binary image with noise.

Figure 1d shows the segmented nuclei along with white areas or points that aren't really nuclei. Those noisy regions were removed by morphological filters [23], such as opening, closing and filling holes operations (see Figure 2).

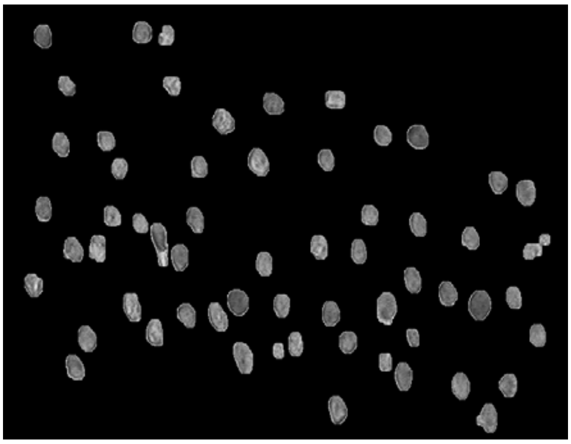

Figure 2. Segmented nuclei superimposed to the original greyscale image.

2.2 Feature extraction

Thirty four (34) morphological and textural features were computed from the nuclei. Table 1 presents the ten (10) morphological features extracted [23]. Table 2 shows the four (4) features based on nuclei histogram, five textural features computed by the co-occurrence matrix [24] and the five features calculated by the run-length matrix [25]. For the ten textural features four orientations were accounted (0°, 45°, 90°, and 135°) and the average and range was calculated leading to eighteen (20) textural features. Each case was represented by one to three images. For each image an average of 60 nuclei were segmented. Thus, the mean value of each feature was computed from all the available nuclei for each case.

The discriminatory power of each feature was assessed by the Wilcoxon statistical test [26]. Thus, only those features that appeared significant statistically differences (*p<0.01*), between low and high grade cases, were further accounting for the design of the proposed system.

Morphological features	
Area	Eccentricity
Orientation	Diameter
Perimeter	Extent
Solidity	Length of Major Axis
Convex Area	Length of Minor Axis

Table 1. Morphological features computed from nuclei.

Textural features		
Image histogram	**Co-occurrence matrix**	**Run-Length matrix**
Mean Value	Contrast	Short-Run Emphasis
Variance	Correlation	Long-Run Emphasis
Skewness	Energy	Gray-level non-uniformity (GLNU)
Kurtosis	Homogeneity	Run-Length non-uniformity (RLNU)
	Entropy	Run-percentage

Table 2. Textural features computed from nuclei.

2.3 System design and evaluation

Five different classifiers namely the Linear Discriminant Analysis (LDA) [27], the Naive Bayes [27], the k-Nearest Neighbor (k-NN) [27], the Support Vector Machine (SVM) [27], and the Probability Neural Network (PNN) [28] were tested for their classification accuracy, sensitivity (prediction of high grade cases accuracy), and specificity (prediction of low grade cases accuracy) in categorizing the cases as low or high grade. Those classifiers were also combined in an ensemble multi-classifier scheme, taking as decision the majority rule. For each classifier, the best feature combination was found by exhaustively search. The system evaluation was performed by applying the Leave One Out (LOO) method. System's generalization performance to unseen data was evaluated by the External Cross Validation method (ECV) [27], where the 70% of the cases were used for the system design (finding the best feature combination by LOO method) and the rest 30% were used for system evaluation.

3 RESULTS AND DISCUSSION

The proposed segmentation technique achieved 80%-85% extraction of all nuclei, and required only 19 seconds for each image to execute. Six morphological (Area, Perimeter, Solidity, Convex Area, Diameter and Length of Major Axis) and four textural features (Mean Value, Skewness, Correlation and RLNU) were found having statistically significant differences (*p<0,001*) between low and high grade cases.

Classifiers	Accuracy (%)	Sensitivity (%)	Specificity (%)
k-nn	87.5	68.4	94.5
Bayesian	87.5	73.6	94.5
SVM	85.7	63.1	97.3
LDA	91	78.9	97.3
PNN	91	78.9	97.3

Table 3. Performance evaluation with the LOO method

Table 3 shows the classifiers performance in terms of the overall accuracy, sensitivity and specificity when the system was evaluated by the LOO method. LDA and PNN classifiers have scored 91% overall accuracy, characterizing correctly the 51 of 56 cases.

The sensitivity of both the LDA and PNN classifiers was 78.9%, which means that 4 of the 19 high grade patterns were misclassified. The specificity was measured 97.3%, which means that only one from 37 low grade cases was misclassified. The optimum features combination, which gave the maximum overall classification accuracy, was the Diameter, the Mean Value, the Skewness, and the RLNU for the LDA classifier, and the Convex Area and the Diameter for the PNN classifier.

The ensemble multi-classifier scheme achieved 91% overall accuracy when the classifiers were combined by 3. The PNN classifier was participated in all three combinations that gave the maximum performance.

Classifiers	Accuracy (%)	Sensitivity (%)	Specificity (%)
k-nn	86.1	66.6	95.8
Bayesian	87.5	75	93.7
SVM	87.4	66.6	97.9
LDA	88.8	75	95.8
PNN	68	45	79.1

Table 4. System’s generalization ability employing the ECV method.

Table 4 shows the generalization performance of the examined classifiers when the ECV method was employed. After ten randomly split of our data (in training and test sets) for ECV evaluation, the LDA classifier achieved a mean overall accuracy of 88.8%. The Solidity and Convex Area were found the most frequently appearing features among the ten best-feature-combinations of the ECV method. The specificity of the system in identifying low grade cases was remarkable and came up to 95.8% in average. Our results indicate that the proposed pattern recognition system may be of value, as a second opinion tool to the physician’s diagnosis in categorizing low and high grade urinary bladder tumours.

REFERENCES

[1] Parkin, D.M., Whelan, S.L., Felay, J. (2002), “Cancer Incidence in Five Continents”, Lyon, France, IARC Publications, Volume VIII (No. 155).

[2] Ferlay, J., Bray, F., Pisani, P. and Parkin, D.M. (2001), *GLOBOCAN 2000 Cancer Incidence, Mortality and Prevalence Worldwide,* IARC Press Version Lyon, France.

[3] Kirkali, Z., Chan, T., Manoharan, M., Algaba, F., Busch, C., Cheng, L., Kiemeney, L., Kriegmair, M., Montironi, R., Murphy, W.M., Sesterhenn, I.A., Tachibana, M., and Weider, J. (2005), “Bladder cancer: Epidemiology, staging and grading, and diagnosis”, Urology, 66 (6), pp. 4-34.

[4] Eble, J.N., Sauter, G., Epstein, J.I. and Sesterhenn, I.A. (2004), *Pathology and Genetics: Tumours of the Urinary System and Male Genital Organs*, World Health Organization Classification of Tumors series, IARCC Publishing, Lyon, France.

[5] Epstein, J.I., Amin, M.B., Reuter, V., Mostofi, F.K., (1998), “The World Health Organization/International Society of Urologic Pathology consensus classification of urothelial (transitional cell) neoplasms of the urinary bladder”, Bladder Consensus Conference Committee Am J Surg Pathol, 22, pp. 1435-1448.

[6] Chaudhuri, B., Rodenacher, K., Burger, G., (1988), “Characterization and featuring of histological section images”, Pattern Recognition Letters, 7, pp. 245–252.

[7] Young, I.T., Sudar, D.,(1988), “Characterization of tissue architecture”, Abstracts of the XIIth International Meeting of the Society for Analytical Cytology, Breckenridge, Colorado, Cytometry Supplement 2, pp. 571.

[8] Choi, H.K., Vasko, J., Bengtssone, E., Jarkrans, T., Malmstrom, P.U., Wester, K., Busch, C., (1994), “Grading of transitional cell bladder carcinoma by texture analysis of histological sections”, Analytical Cellular Pathology, 6, pp. 327–343.

[9] Jarkrans, T., Vasko J, Bengtssone E., Choi, H.K., Malmstrom, P.U., Wester, K., Busch, C. (1995), “Grading of transitional cell bladder carcinoma by image analysis of histological sections”, Analytical Cellular Pathology, 18, pp. 135–158.

[10] Pauwels, R.P.E, Schapers, R.F.M, Smeets, A.W.G.B, Debruyne, F.M.J, Geraedts, J.P.M. (1988), “Grading in Superficial Bladder Cancer. (1) Morphological Criteria”, British Journal of Urology, 61, pp. 129-134.

[11] Velthoven, R., Petein, M., Zlotta, A., (1994), “Computer-assisted chromatin texture characterization of Feulgen-stained nuclei in a series of 331 transitional bladder cell carcinomas”, Journal of Pathology, 173, pp.

235-242.
[12] Murphy, M.W., Soloway, S.M., Jukkola, A.F., Crabtree, N.W, Ford, S.K, (1984), "Urinary Cytology and Bladder Cancer", Cancer, pp. 1555-1565.
[13] Fukuzawa, S., Hashimura, T., Sasaki, M., Yamabe, H., Yoshida, O., (1995), "Nuclear morphometry for improved prediction of the prognosis of human bladder carcinoma", Cancer 10, pp.1790-6.
[14] Lipponen, P.K, Eskelinen, M.J., Kiviranta, J., Nordling, S., (1991), "Classic Prognostic Factors, Flow Cytometric Data, Nuclear Morphometric Variables and Mitotic Indexes as Predictors in Transitional Cell Bladder Cancer", Anticancer Research 11, pp. 911-916.
[15]. Bergvist, A., Ljungqvist, A., Moberger, G., (1965), "Classification of bladder tumours based on the cellular pattern: a preliminary report of a clinical-pathological study of 300 cases with a minimum follow-up of eight years", Acta Chirourgica Scandinavica, 130, pp. 371–378.
[16] Murphy, W. M., Beckwith, J. B., Farrow, G.M. (1994), "Tumours of the kidney, bladder, and related urinary structures", *Atlas of tumour pathology*, 3rd edition, Armed Forces of Institute of Pathology, Washington.
[17] Jonathan, I.E., Mahul, B.A., Victor, R.R, Mostofif, K. (1998), "The World Health Organization/ International Society of Urological Pathology Consensus Classification of Urothelial (Transitional Cell) Neoplasms of the Urinary Bladder", The American Journal of Surgical Pathology, 22, pp. 1435–1448.
[18] Spyridonos, P., Cavouras, D., Makris V., Zenebissis, G., Maratou, V., Kagadis, G.C., Ravazoula, P. and Nikiforidis G.C. (2001), "A Neural Network based segmentation", *IX Mediterranean Conference on Medical and Biological Engineering and Computing*, pp. 546-549.
[19] Spyridonos, P., Ravazoula, P., Cavouras, D., Berberidis, K., and Nikiforidis, G. (2001), "Computer-based grading of heamatoxylin-eosin stained tissue sections of urinary bladder carcinomas", Medical Informatics & the Internet in Medicine, 26, pp. 179–190.
[20] Glotsos, D., Spyridonos, P., Cavouras, D., Ravazoula, P., Arampantoni Dadioti, P., and Nikiforidis, G. (2004), "Automated Segmentationof Routinely Hematoxylin-Eosin-Stained Microscopic Images by Combining Support Vector Machine Clustering and Active Contour Models", Analytical and Quantitative Cytology and Histology, 26 (6), pp. 331-40.
[21] Dunn, J.C. (1973), "A Fuzzy Relative of the ISODATA Process and Its Use in Detecting Compact Well-Separated Clusters", Journal of Cybernetics, 3, pp. 32-57.
[22] Bezdek, J.C. (1981), *Pattern Recognition with Fuzzy Objective Function Algoritms*, Plenum Press, New York.
[23] Wolberg, W.H., Street, W.N. and Mangasarian, O.L., (1999), "Importance of nuclear morphology in breast cancer prognosis", Clin Cancer Res, 5, pp. 3542-8.
[24] Haralick, R.M., Shanmugam, K. and Dinstein, I. (1973), "Textural features for image classification", IEEE Transactions on Systems, Man and Cybernetics, 3, pp. 610-621.
[25] Galloway, M.M. (1975), "Texture Analysis Using Grey Level Run Lengths", Computer Graphics and Image Processing, 4, pp. 172-179.
[26] Soong, T.T. (2004), *Fundamentals of Probability and Statistics for Engineers*, John Wiley & Sons , Chichester, West Sussex, England.
[27] Theodoridis, S. and Koutroumbas, K., (2003), *Pattern Recognition*, Elsevier, San Diego.
[28] Specht, D. (1980), "Probabilistic neural networks", Neural Networks, 3, pp. 109-118.